

International Atomic Energy Agency

INDC(CCP)-372

Distr.: L

INDC

INTERNATIONAL NUCLEAR DATA COMMITTEE

**DETERMINATION OF NEUTRON RESONANCE PARAMETERS
WITH THE IBR-30 PULSED NEUTRON SOURCE FOR
U-238 AND Sm ISOTOPES**

Two papers translated from
Yadernye Konstanty 1991/92

Translated by the IAEA

July 1994

IAEA NUCLEAR DATA SECTION, WAGRAMERSTRASSE 5, A-1400 VIENNA

Reproduced by the IAEA in Austria
July 1994

INDC(CCP)-372

Distr.: L

**DETERMINATION OF NEUTRON RESONANCE PARAMETERS
WITH THE IBR-30 PULSED NEUTRON SOURCE FOR
U-238 AND Sm ISOTOPES**

Two papers translated from
Yadernye Konstanty 1991/92

Translated by the IAEA

July 1994

CONTENTS

Measurement and Analysis of the Resonance Structure	1
Characteristics of the Total Cross-Section and the Radiative Capture Cross-Section of Uranium-238 in the 0.465-200 keV Energy Range	

Yu.V. Grigor'ev, V.N. Koshcheev, G.N. Manturov and
V.V. Sinitsa, Obninsk
Yu.S. Zamyatnin, Dubna
G.V. Muradyan, Moscow
N.B. Yaneva, G.P. Georgiev, B.I. Ivanov and
I.A. Sirakov, Sofia, Bulgaria
(Translated from Yadernye Konstanty 4 (1991), p. 26-39)

Determination of Neutron Resonance Parameters for	19
¹⁴⁷ Sm and ¹⁴⁸ Sm	

G. Georgiev, Yu.S. Zamyatin, L.B. Pikel'ner, Dubna
G.V. Muradyan, Moscow
Yu.V. Grigor'ev, Obninsk
T. Madzharskiy, N. Yaneva, Sofia, Bulgaria
(Translated from Yadernye Konstanty 2 (1992), p. 75-85)

UDC 621.039.51

**MEASUREMENT AND ANALYSIS OF THE RESONANCE STRUCTURE
CHARACTERISTICS OF THE TOTAL CROSS-SECTION AND THE
RADIATIVE CAPTURE CROSS-SECTION OF URANIUM-238
IN THE 0.465-200 keV ENERGY RANGE**

Yu. V. Grigor'ev, V.N. Koshcheev, G.N. Manturov and V.V. Sinita
Institute of Physics and Power Engineering
Obninsk

Yu.S. Zamyatnin
Joint Nuclear Research Institute
Dubna

G.V. Muradyan
I.V. Kurchatov Institute of Atomic Energy
Moscow

N.B. Yaneva, G.P. Georgiev, B.I. Ivanov and I.A. Sirakov
Institute for Nuclear Research and Nuclear Power
Sofia, Bulgaria

ABSTRACT

Using the time-of-flight method on the IBR-30 pulsed neutron source in the 0.465-200 keV energy range, measurements were carried out to determine the total transmissions and the self-indication functions in the radiative capture cross-section for metallic samples of ^{238}U of various thickness. For radiative capture the dependence of the measured data on the multiplicity of registration of gamma rays was investigated. From the experimental data the authors derived the group-averaged total cross-sections (for the BNAB data system) and also the resonance self-shielding factors of the total and radiative capture cross-sections. The average resonance parameters - the neutron and radiative strength functions and scattering radii - were evaluated with the aid of the EVPAR program. The results are compared with other data.

Introduction

In the unresolved resonance region, direct information on the resonance structure of neutron cross-sections may be obtained from the experimental average cross-sections and the total and partial transmission functions. These important integral characteristics of the cross-sections can be used to determine more accurately the average resonance parameters (strength functions and scattering radii) and obtain the resonance self-shielding factors of cross-sections in the BNAB system of group constants [1,2] which is used in practical nuclear reactor and radiation protection calculations. However, in order to measure the transmission, high-intensity sources, high-efficiency detectors and massive thick filter samples are required. Consequently, experiments of this kind have not been very widely performed to date. At this point in time, only the total transmissions in uranium-238 samples have been adequately measured (over 10 papers). References [3, 4], which present results for the temperature dependence of transmission values, are worthy of note. The partial transmissions for the radiative capture and scattering cross-sections (these are also called self-indication functions) have also been measured and are presented in Refs [4-9]. However, these transmission data were mainly obtained using thin filter samples and a small range of thicknesses. Unfortunately, the divergences between the results in these papers go beyond the limits of experimental error and their interpretation is not unique. Since uranium-238 is a very important reactor raw material, the nuclear physics constants for it need to be refined using an improved experimental technique. We therefore measured the total transmissions and self-indication functions in ^{238}U radiative capture on the 1000-metre path length of the IBR-30 pulsed fast reactor using an all-wave neutron detector with ^3He counters [5] and a gamma-ray scintillation detector with NaI(Tl) crystals [10] operating in multiple registration mode. From the experimental transmissions we obtained the resonance

self-shielding factors and determined the average resonance parameters in the unresolved energy region.

Experimental methodology

The measurements were carried out using the IBR-30 facility operating in booster mode with a multiplication coefficient of 200 at a mean thermal power of 10 kW, a neutron burst length at half-maximum of 4 μ s, and a burst frequency of 100 Hz. The total and partial transmissions were measured simultaneously in good geometry conditions for an energy range of 0.1-200 keV. The neutron detector, consisting of an annular battery of 16 type SNM-18 ^3He counters, was situated 1006 m from the neutron source and a scintillation detector with 16 NaI(Tl) crystals was located at 502 m. The filter samples, made of metallic ^{238}U , in the form of discs 195 mm in diameter and of varying thickness, were placed in the neutron beam 242 m from the neutron source. Both detectors (for registering neutrons and gamma rays) have apertures to accept the radiator samples, cover a solid angle of almost 4π -steradian, and have a radiation registration efficiency of 6% and 80% respectively when the signal pulse registration thresholds are optimal. To measure the total transmissions, a polyethylene disc 80 mm in diameter and 10 mm thick was used as a radiator sample and, to measure the partial capture transmissions, thin samples of metallic ^{238}U 0.00238 nuclei/b thick and 80 mm in diameter or an equivalent background scatterer sample made of natural lead 0.00316 nuclei/b thick and 80 mm in diameter were placed inside the gamma-ray detector. To reduce the background, cadmium and boron carbide filters were placed permanently in the neutron beam, in order to eliminate recycling neutrons. Apart from the external shielding, the gamma-ray detector had an internal shield - a paraffin and boron carbide converter with an overall thickness of 65 mm - and a vacuum tube was inserted in the aperture. Two monitor counters, located 60 m from the source,

were used to monitor the source strength. All the information from the detectors and monitors in the form of time spectra (one from the neutron detector and 16 multiplicities from the gamma-ray detector) was stored in the measuring module [11] which processed the spectra and produced the transmissions at the same time as the measurements were being taken.

Measurement results

During the measurement process, time spectra were accumulated with filter samples of seven different thicknesses in the neutron beam and without any filter samples in the beam for an energy range of 110 eV-10 MeV. These spectra were compressed into the smallest number of channels within the limits of the energy groups of the BNAB system of constants. The transmissions were determined in the form of the integral characteristics of the cross-sections:

$$T_x(n) = \frac{N(n) - \{F_v(n) + F_c(n)\}}{N(0) - \{F_v(0) + F_c(0)\}} \cdot \frac{M(0)}{M(n)} = \int_{\Delta E} \varphi(E)\varepsilon(E)e^{-\sigma_t(E)n} dE / \int_{\Delta E} \varphi(E)\varepsilon(E) dE, \quad (1)$$

where $T_x(n)$ is the total transmission or self-indication function for a sample of thickness n ; $\varphi(E)$ is the neutron beam spectrum; $\varepsilon(E)$ is the detector efficiency; $\sigma_t(E)$ is the total cross-section; $N(n)$ and $N(0)$ are the detector counts with the filter sample in and out of the beam respectively; $F_v(n)$ and $F_v(0)$ are the variable background components; $F_c(n)$ and $F_c(0)$ are the constant background components; and $M(n)$ and $M(0)$ are the monitor counts.

Equation (1) may be used both to determine the total transmissions and the self-indication functions. In the latter case, the detector efficiency is proportional to the radiative capture cross-section, which implies that the resonance cross-section self-shielding will be enhanced. The constant background level in the spectra was determined using the

lower resonances of tungsten and cadmium, samples of which were permanently placed in the neutron beam.

When measuring spectra using the gamma ray detector for a specific filter sample thickness, the variable background components were determined with the aid of an equivalent lead scatterer according to the formula:

$$F_v = N(Pb) \frac{n(U)}{n(Pb)} \cdot \frac{\sigma_s(U)}{\sigma_s(Pb)} \cdot \frac{T_s(U)}{T(U)_s} \cdot \frac{M(U)}{M(Pb)_t}, \quad (2)$$

where $N(Pb)$ is the number of neutrons registered which were scattered by the lead sample; $n(U)$ and $N(Pb)$ are the numbers of nuclei per cm^2 for the uranium and lead radiator sample; $\sigma_s(U)$ and $\sigma_s(Pb)$ are the mean scattering cross-sections for uranium and lead respectively; $T_s(U)$ is the partial transmission of the uranium scattering cross-section; $T_t(U)$ is the total transmission for uranium; $M(U)$ and $M(Pb)$ are the monitor counts in the measurements with the uranium and lead radiator sample.

The variable background was also determined using aluminium (35; 85; 140 keV) and manganese (0.337; 2.4 keV) resonance filters in the total and partial transmission measurements.

Since the time spectra of all the multiplicities from the 1st to the 16th were measured simultaneously with the gamma-ray detector, the partial transmissions were also obtained for all the multiplicities and for the sum channel. It should be noted that the background components in the spectra decrease as the multiplicity increases. For instance, in spectra of the third multiplicity the background level is 10-100% lower than in the sum spectra. The background levels increase with decreasing energy and increasing filter sample thickness within a range of 10-95% with a background determination accuracy of approximately 3%

and 0.5% respectively. The background in the neutron detector spectra did not exceed 15% over a wide energy range and was only slightly dependent on the filter sample thickness.

The experimental transmissions obtained are shown in Table 1. The errors in the transmissions amount to 1-2% for small attenuations and reach 10-30% for transmissions of 0.1-0.05. Figure 1 shows the self-indication functions for various multiplicities and they agree within the error limits.

Analysis of measurement results

At high energies, the total and partial transmissions agree within the limits of experimental error, which indicates that there are no resonance self-shielding effects in the radiative capture cross-section. The non-exponential shape of the total transmissions indicates that there is resonance blocking of the total cross-section in all the energy groups shown. There is good agreement between the total transmissions obtained here and in the investigation performed in Ref. [14] on the same 1000-metre path length of the IBR-30 but with a different detector and an inferior energy resolution (the neutron burst length was 100 μ s). This may be clearly seen in Figs 2-4 which show the observed cross-sections $\sigma_{to} = -\frac{1}{n} \ln T$ for various filter sample thicknesses as a function of neutron energy. For large filter sample thicknesses, the observed total cross-sections tend to a constant value which is close to the potential scattering cross-section.

By extrapolating the cross-sections given in the region of small filter sample thicknesses, the average cross-sections at zero thickness can be determined. However, this procedure is very indeterminate owing to the high experimental errors at $T \approx 1$. Therefore, the method of subgroup representation of the mean cross-sections and functionals such as the transmissions and the resonance self-shielding factors is more acceptable [12]. In this

instance, the experimental transmissions are approximated by the sum of the exponential functions. Only two exponents are required to describe the transmissions in this experiment:

$$T_t(n) = a_1 e^{-\sigma_{t1} n} + (1 - a_1) e^{-\sigma_{t2} n}; \quad \langle \sigma_t \rangle = a_1 \sigma_{t1} + (1 - a_1) \sigma_{t2}, \quad (3)$$

$$T_\gamma(n) = a_{\gamma 1} e^{-\sigma_{\gamma 1} n} + (1 - a_{\gamma 1}) e^{-\sigma_{\gamma 2} n}; \quad \langle \sigma_\gamma \rangle = a_{\gamma 1} \sigma_{\gamma 1} + (1 - a_{\gamma 1}) \sigma_{\gamma 2}, \quad (4)$$

$$f(\sigma_o) = \frac{1}{\langle \sigma_t \rangle} \left[\frac{a_1 / (\sigma_{t1} + \sigma_o) + (1 - a_1) / (\sigma_{t2} + \sigma_o)}{a_1 / (\sigma_{t1} + \sigma_o)^2 + (1 - a_1) / (\sigma_{t2} + \sigma_o)^2} - \sigma_o \right], \quad (5)$$

$$f_\gamma(\sigma_o) = \frac{a_{\gamma 1} / (\sigma_{\gamma 1} + \sigma_o) + (1 - a_{\gamma 1}) / (\sigma_{\gamma 2} + \sigma_o)}{a_1 / (\sigma_{t1} + \sigma_o) + (1 - a_1) / (\sigma_{t2} + \sigma_o)}, \quad (6)$$

where a_1 , $a_{\gamma 1}$ are the contributions of the first subgroup cross-sections; σ_{t1} , σ_{t2} , $\sigma_{\gamma 1}$, $\sigma_{\gamma 2}$ are the subgroup cross-sections; σ_o is the dilution cross-section; and $f_t(\sigma_o)$, $f_\gamma(\sigma_o)$ are the resonance self-shielding factors of the total cross-section and the radiative capture cross-section.

The optimum subgroup parameters were found using the method of least squares. Table 2 gives the mean group cross-sections obtained in the experiment and data from other sources.

The experimental total cross-sections in all the works cited [9, 13, 14] agree with the data in this paper within the error limits, as do the evaluated data in Ref. [2]. However, there is a marked trend towards higher cross-section values in this paper and in the experiment reported in Ref. [14] which was also performed using the 1000-metre path length of the IBR-30. In addition, it should be noted that the experimental data in Ref. [13] were obtained from total transmissions measured using monoenergetic neutrons with an energy resolution of approximately 60% at 10 keV and 10% at 200 keV, a set of filter samples

with thicknesses ranging from 3 to 250 mm, and a measurement aperture several orders of magnitude smaller than in our experiment. These features of experiments [9] and [13] could result in the transmissions being too high and, correspondingly, the average group cross-sections being too low.

Apart from the total cross-sections, the resonance self-shielding factors of the ^{238}U neutron cross-sections were obtained from the subgroup parameters derived from the transmissions. The results of this treatment and data from other sources are shown in Table 3. The data obtained by different authors from the same basic transmissions using different methods are worthy of note. Thus, the results in Refs [14] and [15] differ by 30% in some energy groups, even though the original data were identical. Clearly, these divergences are caused by the fact that, in Ref. [14], the self-shielding factors were determined using the subgroup method, whereas in Ref. [15] they were determined using the average resonance parameters. In Ref. [15], lower values were also obtained for the average group total cross-sections compared with Ref. [14].

As can be seen from Table 3, the experimental resonance self-shielding factors from the present investigation agree within the limits of experimental error with the experimental data in Ref. [9] and do not contradict the results of the evaluation in Ref. [2].

The measurement results for the total and capture transmission functions in the 4.65-200 keV energy region were used to evaluate the mean resonance parameters, i.e. the scattering radii, neutron and radiation strength functions. This was done using the EVPAR program [16, 19].

With the EVPAR program, all kinds of experimental data can be taken into account in the evaluation (average, total and partial cross-sections - σ_t , σ_γ , σ_s). The latest version even allows one to take account of the transmission functions, including those measured

using the self-indication method. This program uses Hauser-Feshbach-Moldauer formalism to calculate the average cross-sections. The total and partial transmission functions are calculated in a multi-level approximation which takes account of inter-resonance interference, Doppler broadening of resonances and fluctuations in neutron widths. The parameters of the calculation models used in the EVPAR program are the scattering radii R_l , the neutron strength functions $S_{n,l}$ and the radiation strength functions $S_{\gamma,l}$ for neutron waves with orbital angular momenta $l = 0,1,2$. The maximum likelihood method is used in the program to fit the calculated data to the experimental data. It is important to note that the calculation results in the EVPAR program can be presented in ENDF/B format as a section of the corresponding file with energy-dependent parameters (MF = 2, MT = 151, LRU = 2 - see description of formats in Ref. [17]).

Table 4 shows the average resonance parameters obtained here by fitting the transmission data, and compares them with results from other sources. The values obtained for the strength functions S_{n0} and S_{n1} , and for $\Gamma_{\gamma0}$ and D_0 agree well with the results of averaging the resolved resonance parameters. With regard to the scattering radii R_l , in order to make the data at low and high energies agree, it was necessary to introduce the energy dependence of the parameters R_l' , $R_l = R_l' (1 - 0.2 \times E \text{ MeV})$. Figures 2-4 compare experimental results with calculated curves from the present work. Figure 5 also shows the calculated energy dependences of the total and radiative capture cross-sections for ^{238}U in comparison with the experimental data. Table 3 presents the self-shielding factors which were calculated with the GRUKON program [18] from the evaluated mean resonance parameters. They are very similar to the results in Ref. [15].

In conclusion, it should be noted that the mean resonance parameters, cross-sections and resonance self-shielding factors obtained from the transmissions agree with the evaluations in other works and can be used to refine the neutron constants for ^{238}U .

REFERENCES

- [1] ABAGYAN, L. P., BAZAZYANTS, N. O., BONDARENKO, I. I., NIKOLAEV, M. N., Group Constants for Nuclear Reactor Calculations, Atomizdat, Moscow (1964) [in Russian].
- [2] ABAGYAN, L. P., BAZAZYANTS, N. O., NIKOLAEV, M. N., TSIBULYA, A. M., Group Constants for Reactor and Shielding Calculations, Ehnergoizdat, Moscow (1981) [in Russian].
- [3] VAN'KOV, A. A., GRIGOR'EV, Yu. V., NIKOLAEV, M. N., et al., Proc. Conf. on Nuclear Data for Reactors, Helsinki, Vol. 1, IAEA, Vienna (1970) 559.
- [4] BYOUN, T. Y., BLOCK, R., SEMLER, T., Proc. Nat. Top. Meet. on New Developments in Reactor Physics and Shielding, USAEC, New York (September 1972) 115.
- [5] GRIGOR'EV, Yu. V., BAKALOV, T., ILCHEV, G., Measurement of Resonance Self-Shielding Effects of the Scattering Cross-Section in the 1-100 keV Neutron Energy Region, Preprint FEhI-1216 [Institute of Physics and Power Engineering], Obninsk (1981) [in Russian].
- [6] PEREZ, R. B., DE SAUSSURE, G., YANG, T., et al., Trans. Amer. Nucl. Soc. **44** (1983) 337.
- [7] KAZAKOV, L. E., KONONOV, V. N., MANTUROV, G. N., et al., Problems of Nuclear Science and Technology, Series: Nuclear Constants, No. 3 (1986) 37 [in Russian].
- [8] FUJITA, I., KOBOYASHI, R., KOMAMOTO, S., et al., Neutron Physics (Proc. 1st Int. Conf. on Neutron Physics), Vol. 2, Kiev-Moscow (1988) 195 [in Russian].
- [9] BOKHOVKO, M. V., KONONOV, V. N., MANTUROV, G. N., et al., Problems of Nuclear Science and Technology, Series: Nuclear Constants, No. 3 (1988) 11 [in Russian].
- [10] GEORGIEV, G. P., GRIGOR'EV, Yu. V., ERMAKOV, V. A., et al., Facility for Measuring Neutron Cross-Sections and Radiation Multiplicity during Interaction of Neutrons with Nuclei, Report OIYaI R3-88-555 [Joint Nuclear Research Institute], Dubna (1988) [in Russian].

- [11] GRIGOR'EV, Yu. V., SIRAKOV, I. A., KHRYKINA, T. D., TISHIN, V. G., Measuring Module with the "FORD" Control Program for Investigating the Resonance Structure of Neutron Cross-Sections, Preprint FEH-2060, Obninsk (1989) [in Russian].
- [12] NIKOLAEV, M. N., KHOKHLOV, V. F., Bulletin of the Nuclear Data Information Centre 4 (1967) 420 [in Russian].
- [13] FILIPPOV, V. V., Problems of Nuclear Science and Technology, Series: Nuclear Constants, No. 4 (1985) 33 [in Russian].
- [14] GRIGOR'EV, Yu. V., Measurement of the Neutron Cross-Sections and Resonance Characteristics of ^{238}U on the IBR spectrometer, author's abstract of dissertation for Candidate degree, OIYaI, Dubna (1980) [in Russian].
- [15] VAN'KOV, A. A., UKRAINTSEV, V. F., Problems of Nuclear Science and Technology, Series: Nuclear Constants, No. 4 (1987) 58 [in Russian].
- [16] MANTUROV, G. N., NIKOLAEV, M. N., Neutron Physics (Proc. 1st Int. Conf. on Neutron Physics), Vol. 1, Kiev-Moscow (1988) 440 [in Russian].
- [17] ENDF-102, Data Formats and Procedures for the Evaluated Nuclear Data File, ENDF/B-V, BNL-NCS-50496 (1983).
- [18] SINITSA, V. V., Problems of Nuclear Science and Technology, Series: Nuclear Constants, No. 5 (59) (1984) 34 [in Russian].
- [19] MANTUROV, G. N., LUNEV, V.P., GORBACHEVA, L. V., Neutron Physics (Proc. 6th All-Union Conf. on Neutron Physics), Vol. 2, Moscow (1983) 231 [in Russian].
- [20] VAN'KOV, A. A. , GOSTEVA, L. S. , UKRAINTSEVA, V. F. , Problems of Nuclear Science and Technology, Series: Nuclear Constants, No. 3 (1983) 27 [in Russian].

Table 1

Total and partial transmission levels for ^{238}U

Group No.	E_{ν} (keV)	n (mm)	1	2	4	8	16	32	64
		n (nuclei/b)	0,00478	0,00958	0,0190	0,0380	0,0764	0,153	0,306
8	200- 100	T_t [14]	-	-	-	-	-	-	-
		T_t	0,961	0,887	0,812	0,668	0,456	0,209	0,045
		T_{γ}	0,959	0,901	0,830	0,666	0,446	0,219	0,050
9	100- 46,5	T_t [14]	0,935	0,874	0,800	0,629	0,407	0,174	0,038
		T_t	0,939	0,836	0,757	0,644	0,395	0,162	0,0358
		T_{γ}	0,941	0,901	0,804	0,635	0,424	0,186	0,036
10	46,5-21,5	T_t [14]	0,926	0,866	0,795	0,606	0,373	0,172	0,033
		T_t	0,947	0,861	0,771	0,613	0,387	0,158	0,0358
		T_{γ}	0,916	0,866	0,764	0,589	0,374	0,142	0,030
11	21,5-10	T_t [14]	0,919	0,883	0,786	0,593	0,376	0,162	0,032
		T_t	0,930	0,856	0,758	0,596	0,376	0,156	0,0365
		T_{γ}	0,908	0,847	0,744	0,536	0,331	0,123	0,022
12	10 - 4,65	T_t [14]	0,914	0,855	0,766	0,584	0,362	0,167	0,034
		T_t	0,933	0,850	0,751	0,602	0,371	0,157	0,0378
		T_{γ}	0,922	0,831	0,714	0,519	0,311	0,108	0,023
13	4,65-2,15	T_t [14]	0,914	0,831	0,770	0,560	0,360	0,162	0,045
		T_t	0,908	0,820	0,725	0,581	0,356	0,147	0,0413
		T_{γ}	0,772	0,724	0,556	0,379	0,377	0,050	-
14	2,15- 1,0	T_t [14]	0,898	0,807	0,759	0,591	0,390	0,186	0,054
		T_t	0,897	0,810	0,718	0,584	0,392	0,186	0,0618
		T_{γ}	0,636	0,490	0,371	0,248	0,160	0,040	-
15	1,0-0,465	T_t [14]	-	-	-	-	-	-	-
		T_t	0,930	0,844	0,755	0,592	0,436	0,212	0,0646
		T_{γ}	0,530	0,359	0,304	0,193	0,091	0,039	-

Table 2

Mean group cross-sections $\langle \sigma_t \rangle$ and $\langle \sigma_{t\gamma} \rangle$ for ^{238}U

Group No.	E_g (keV)	exp. $\langle \sigma_t \rangle$	exp. $\langle \sigma_{t\gamma} \rangle$	$\langle \sigma_t \rangle$ [13]	$\langle \sigma_t \rangle$ [9]	$\langle \sigma_t \rangle$ [14]	$\langle \sigma_t \rangle$ [2]
8	200-100	11,5±0,3	10,8±0,3	11,7±0,1	-	12,0±0,5	11,53
9	100-46,5	12,8±0,3	12,0±0,3	12,7±0,1	12,4±0,3	13,0±0,5	12,57
10	46,5-21,5	13,9±0,4	14,2±0,4	13,5±0,2	13,7±0,3	14,6±0,5	13,46
11	21,5-10,0	15,5±0,5	17,5±0,8	14,5±0,2	14,6±0,4	16,5±0,5	14,48
12	10,0-4,65	15,5±0,5	20,1±1,0	16,4±0,3	16,5±0,5	17,3±0,8	15,88
13	4,65-2,15	20,7±0,7	111±11	-	-	20,0±0,8	18,95
14	2,15-1,00	24,0±1,0	112±12	-	-	22,2±1,0	22,19
15	1,0-0,465	24,0±1,0	176±18	-	-	24,0±1,0	23,70

Table 3

Resonance self-shielding factors for the ^{238}U total and radiative capture cross-sections

Group No.	E_g (keV)		Experiment	Calculation	[13]	[9]	[14]	[15]	[2]
8	200 - 100	f_t	0,88±0,04	0,957	0,94	-	-	-	0,950
		f_γ	1,00	0,986	-	-	-	-	0,986
9	100 - 46,5	f_t	0,79±0,04	0,926	0,91	0,946±0,029	0,86±0,04	-	0,915
		f_γ	0,95±0,02	0,962	-	0,980±0,014	-	-	0,958
10	46,5-21,5	f_t	0,77±0,04	0,840	0,83	0,864±0,031	0,82±0,05	0,774	0,855
		f_γ	0,94±0,02	0,914	-	0,931±0,024	-	0,879	0,910
11	21,5-10,0	f_t	0,68±0,04	0,657	0,76	0,777±0,035	0,70±0,05	0,544	0,755
		f_γ	0,84±0,03	0,765	-	0,868±0,035	-	0,781	0,830
12	10,0-4,65	f_t	0,68±0,04	0,588	0,68	0,617±0,044	0,60±0,07	0,472	0,668
		f_γ	0,78±0,04	0,666	-	-	-	0,659	0,719
13	4,65-2,15	f_t	0,51±0,03	-	-	-	0,44±0,10	-	0,447
		f_γ	0,51±0,03	-	-	-	-	-	0,501
14	2,15-1,00	f_t	0,36±0,03	-	-	-	0,39±0,10	-	0,407
		f_γ	0,36±0,02	-	-	-	-	-	0,304
15	1,0-0,465	f_t	0,35±0,03	-	-	-	-	-	0,365
		f_γ	0,24±0,02	-	-	-	-	-	0,183

Table 4

Mean resonance parameters for ^{238}U

Source	$S_{n1} \cdot 10^4$		Γ_γ	D_1 (eV)		R_1 (fm)	
	$l=0$	$l=1$	$l=0$	$l=0$	$l=1$	$l=0$	$l=1$
This work	1,10±0,05	1,70±0,20	23,5±0,7	20,8*	6,9	9,35	8,0
[3]	0,89±0,01	1,87±0,03	24,8*	20,8*	6,9	9,01	9,01
[19]	0,93±0,03	2,30±0,07	22,9±0,7	20,8*	4,4	9,35	6,70
[20]	1,14	2,0	22,2	21,6	7,2	9,13	9,13
[7]	1,11±0,11	2,20±0,20	22,9±0,9	20,8*	6,9	-	-

* Parameter fixed during optimization.

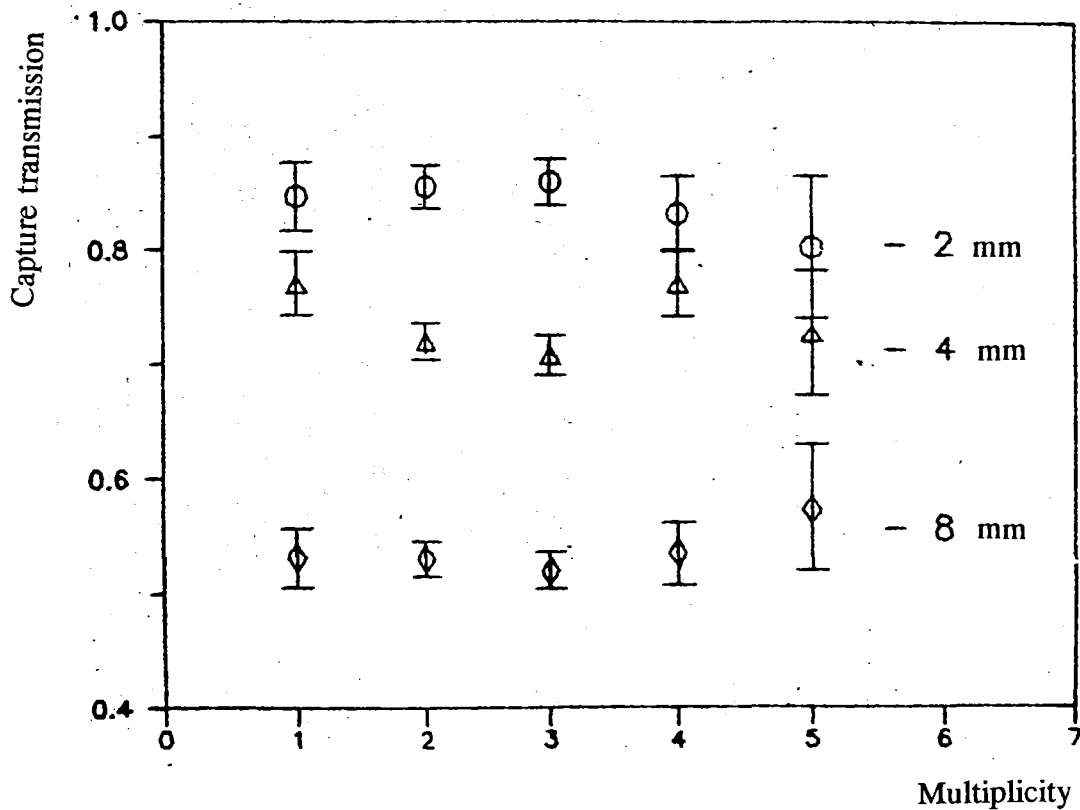
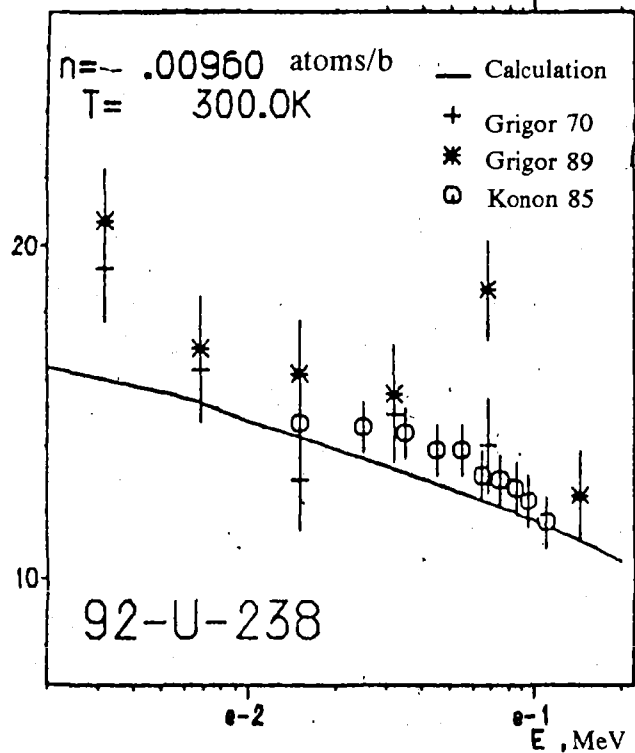
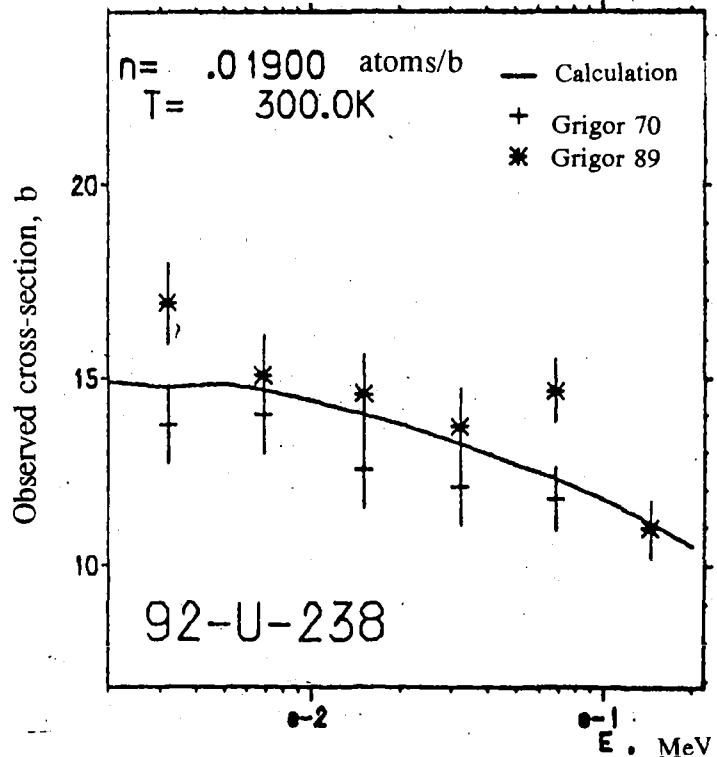


Fig. 1. Dependence of capture transmission in uranium-238 on the gamma-ray registration multiplicity for various filter sample thicknesses.

Total transmission



Total transmission



Observed cross-section, b

Fig. 2. Energy dependence of the observed cross-section for 2 and 4 mm uranium-238 filter samples.

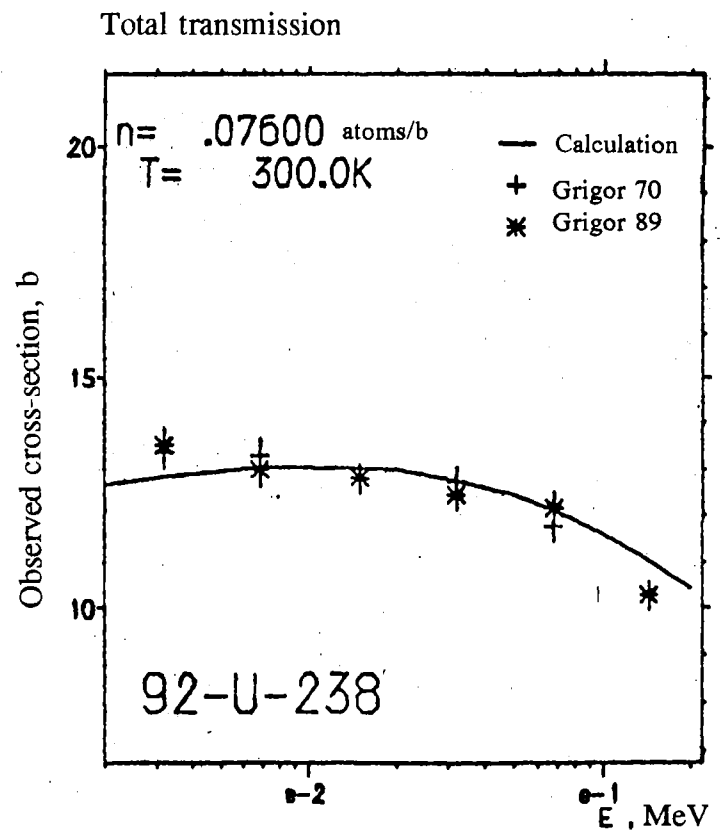
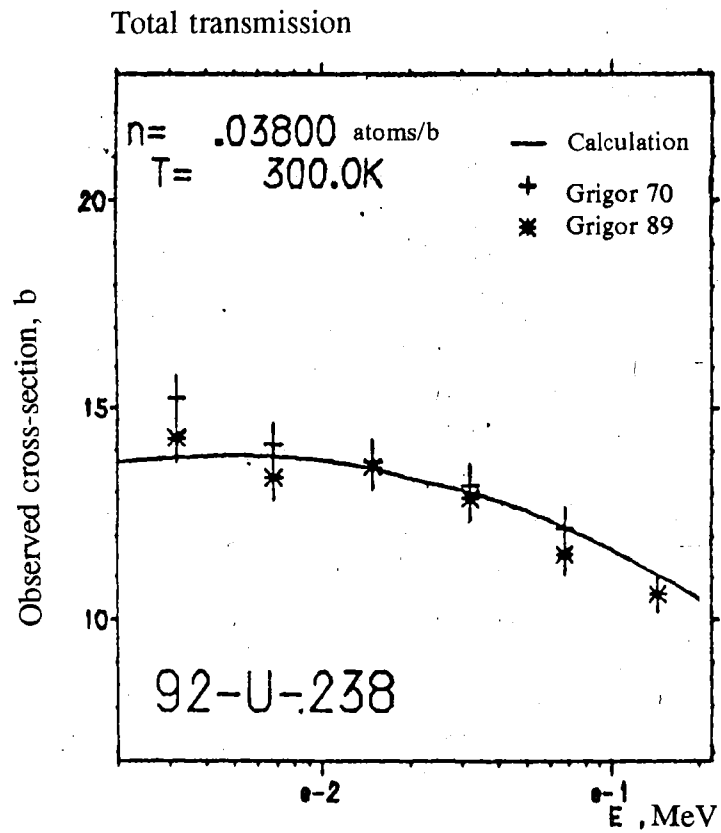
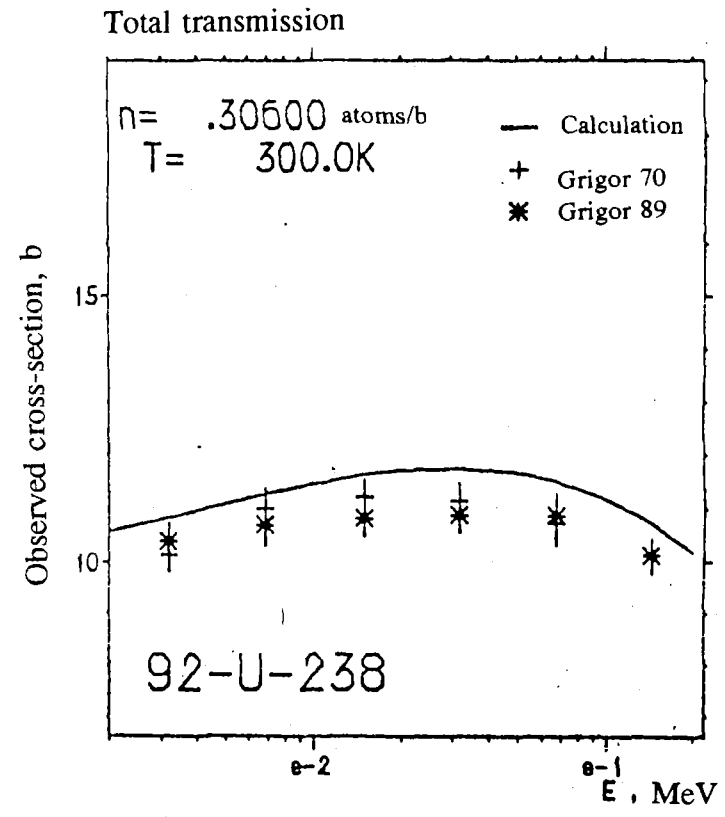
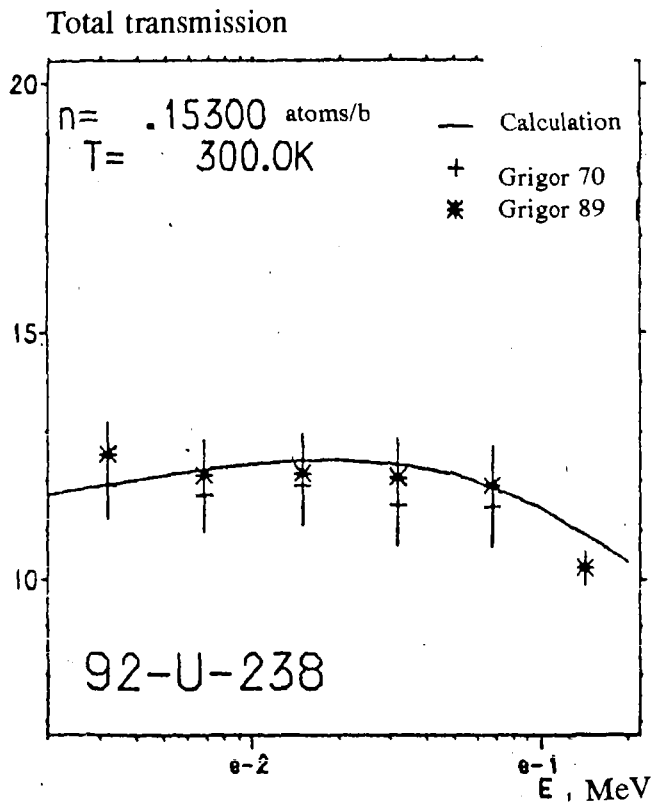


Fig. 3. Energy dependence of the observed cross-section for 8 and 16 mm uranium-238 filter samples.



Observed cross-section, b

Fig. 4. Energy dependence of the observed cross-section for 32 and 64 mm uranium-238 filter samples.

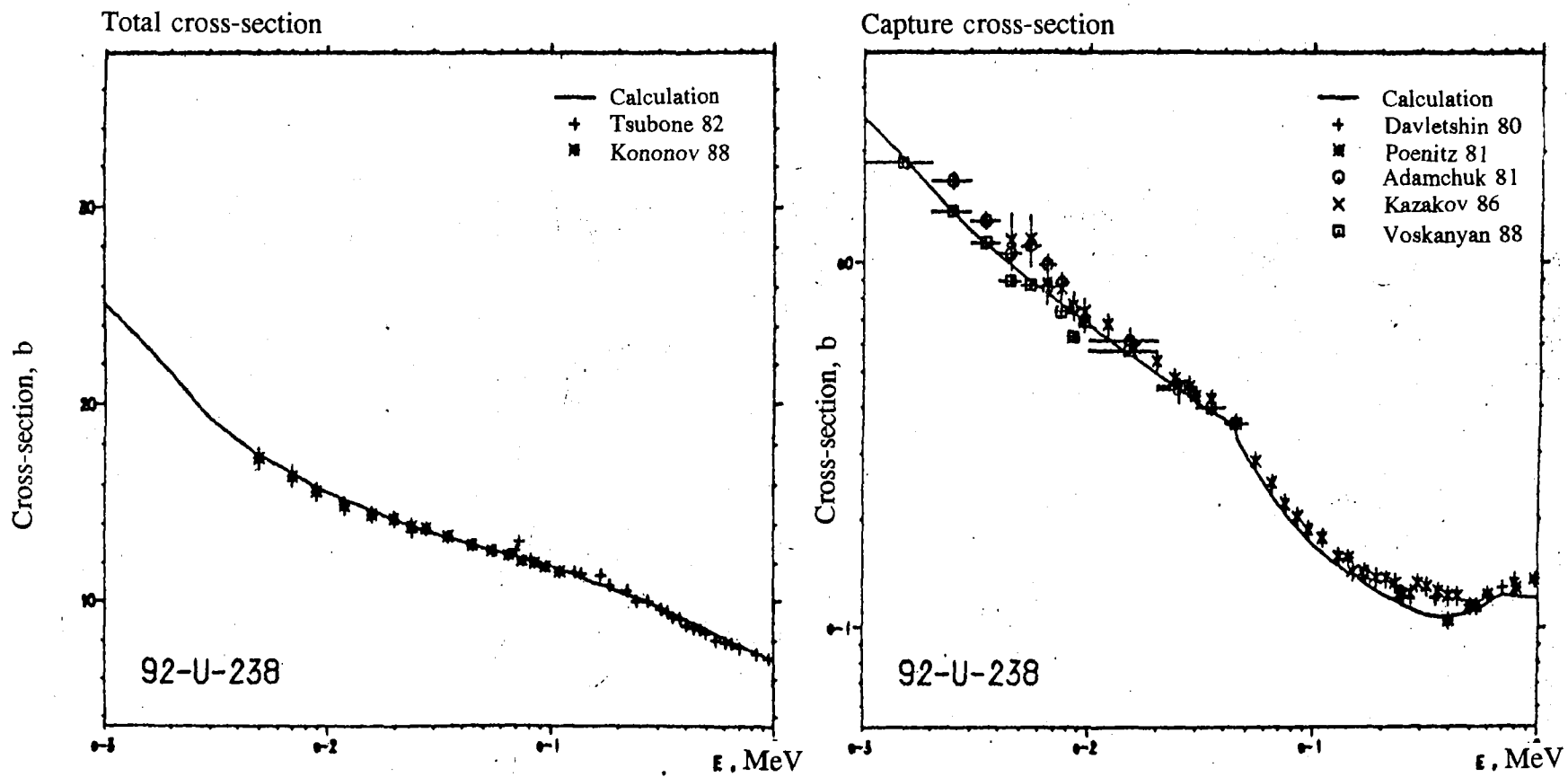


Fig. 5. Total cross-section and radiative capture cross-section for uranium-238 in the 1-1000 keV energy region.

94-10592 (C)
Translated from Russian

UDK 539.172

DETERMINATION OF NEUTRON RESONANCE PARAMETERS
FOR ^{147}Sm AND ^{148}Sm

G. Georgiev, Yu.S. Zamyatin, L.B. Pikel'ner
Joint Nuclear Research Institute, Dubna, Russia

G.V. Muradyan
I.V. Kurchatov Institute of Atomic Energy, Moscow, Russia

Yu.V. Grigor'ev
Institute of Physics and Power Engineering, Obninsk, Russia

T. Madzharskiy, N. Yaneva
Nuclear Research and Power Institute, Sofia, Bulgaria

ABSTRACT

The measurements were performed using the γ -ray multisectional 4π -detector, placed on the 500 m flight path of the pulsed neutron booster IBR-30 of LNP, JINR. The combination of multiplicity spectrometry with the time-of-flight method made it possible to identify γ -capture and scattering events in isolated resonances and to determine spins, and neutron and radiative resonance widths. The measurements made it possible to assign spins for ^{147}Sm resonances up to 900 eV and to determine the neutron strength functions for both spin states. The radiative widths for 25 resonances of ^{147}Sm were determined up to 300 eV. The level positions of 25 resonances in the energy range up to 3 keV and the values of Γ_n and Γ_γ for a number of resonances up to 1.5 keV for ^{148}Sm were obtained.

Introduction

The motivation for studying neutron radiative capture is the fact that this process is not yet completely understood physically and has also still not been fully described theoretically. The application of gamma-ray multiplicity spectrometry in conjunction with the time-of-flight method [1] is producing extensive experimental information on radiative capture in the resonance region of neutron energies and on resonance level characteristics.

When s neutrons are captured by non-zero spin nuclei, the resonance levels of the compound nucleus divide into two groups according to their spin. Since the data on resonance spin are extremely fragmentary, attention is being focused on those gamma-cascade characteristics which demonstrate systematic dependence on the spin of the resonance levels.

In this paper we present the results of a study of the radiative capture of resonance neutrons by the isotopes ^{147}Sm and ^{148}Sm in the resolved resonance region using the multiplicity spectrometry method. These isotopes were chosen for investigation because ^{147}Sm has a ground-state spin of $7/2^-$ and after s -neutron capture forms level systems with spins of 3^- and 4^- . This makes it possible to verify whether there is a correlation between the level spin and gamma-ray characteristics during de-excitation. Furthermore, the radiation widths, which are known for several low energy resonances of this isotope, show significant fluctuations [2]. This means that they need to be validated. In contrast to ^{147}Sm , the even-even isotope ^{148}Sm has a spin of $J = 1/2$ for all the s resonances, but only five of its resonance energy values are known. This made it advisable to acquire more comprehensive information on its resonances, to determine their neutron and radiation widths, to obtain data on its capture gamma rays and to compare them with the data for ^{147}Sm .

The experiment

The measurements were performed with a "Romashka" 4π multisection scintillation detector [1], positioned on the 500 m flight path of the IBR-30 pulsed neutron booster at the Dubna Joint Nuclear Research Institute's Neutron Physics Laboratory. The booster had a capacity of 10 kW and a multiplication factor of 200. The neutron burst lasted about $4\mu\text{s}$, the resolution of the spectrometer was 8 ns/m and the pulse repetition frequency was 100 pulses/s.

The detector had 16 separate sections, each of which consisted of an NaI(Tl) crystal of 122 x 122 x 152 mm, was viewed by its own photomultiplier and had a vacuumized through channel to allow passage of the collimated neutron beam and to enable the samples to be positioned inside the detector (Fig. 1). A more detailed description of the detector and its parameters is given in Ref. [3].

The time-of-flight of the neutron and the gamma-ray coincidence multiplicity were recorded for each neutron capture event. The recording system stored a capture event and its parameters whenever the total energy of the gamma quanta registered by the detector fell within the range of 2-8 MeV. The pulse recording threshold of each detector section was 0.1 MeV.

This type of pulse recording system, combining the time-of-flight method with multiplicity spectrometry, made it possible to measure simultaneously 16 time-of-flight spectra corresponding to the coincidences for different multiplicities and to obtain a three-dimensional representation of the gamma-ray multiplicity distribution for individual resonances (Fig. 2).

Neutron scattering events were recorded at the same time. For this purpose a boron n- γ converter containing a moderator was positioned inside the detector and the scattered neutrons were recorded by registering the single monoenergetic gamma rays with an energy of 0.48 MeV from the $^{10}\text{B}(n,\alpha\gamma)$ reaction. The converter also shielded the detector from the scattered neutrons. It should be noted that this is a very effective method of measuring neutron scattering and that it also extends the range of resonances available for measurement.

The information arriving from the detector was classified, stored and recorded on 16 x 4K files per 2 μs for each channel in a special measuring module.

The samples were arranged in the centre of the detector at a flight distance of 501.9 m. They comprised oxides (Sm_2O_3) of the enriched isotopes ^{147}Sm and ^{148}Sm of two thicknesses, packed into thin-walled aluminium containers of 100 mm in diameter. The isotopic composition and thickness of the samples (according to the isotope being measured) are presented in Table 1.

The neutron flux was monitored using two ^3He SNM-17 counters arranged outside the neutron beam at a distance of 60 m from the source. In order to suppress the background of recycling neutrons, cadmium (1 mm) and boron carbide (10 mm) filters were positioned in the beam throughout the experiment.

Results

Several series of measurements were performed for each sample of samarium. The measurements lasted a total of 168 hours for ^{147}Sm and 171 hours for ^{148}Sm . As an example, Fig. 3 shows parts of the time-of-flight spectra during recording by the detector of quadruple coincidences of capture gamma rays and neutron scattering events for a ^{147}Sm sample with a thickness of 3.45×10^{-4} at/b.

Figure 4 shows the time-of-flight spectra for neutron capture and scattering for ^{148}Sm .

The energy values of the neutron resonances were determined with respect to the reference resonance energies for ^{238}U [2]. By virtue of the consistency in the conditions for measuring the U and Sm samples and the methods used to process the results, the values for Sm resonance energies are virtually free of systematic errors. The resonance energies obtained in the 15-900 eV range for ^{147}Sm and the 15 eV-3 keV range for ^{148}Sm are given in Tables 2 and 3 respectively. As can be seen from Fig. 4, in the energy range indicated, more than 20 resonances of ^{148}Sm are observed. However, owing to poor resolution in the

range above 1 keV, it is not possible to confirm that all the resonances shown for this range are single ones.

(a) Multiplicity spectra and resonance spins

Initial processing of the measurement results made it possible to determine the S_k areas under the resonance peaks for time-of-flight spectra for different values of multiplicity

k , with k ranging from 1 to 7 and to determine the fraction of capture events $p_k = S_k / \sum_k S_k$

corresponding to a simultaneous recording by the detector of k gamma quanta and also the

average multiplicity values $\langle k \rangle = \sum_k k p_k$ for each resonance. The multiplicity distributions

thus obtained for two resonances of ^{147}Sm are presented in Fig. 5. The $\langle k \rangle$ values for the ^{147}Sm resonances are shown in Fig. 6. It can be seen from the diagram that the resonances are divided in terms of the $\langle k \rangle$ values reasonably clearly into two groups corresponding to spin values of 3^- and 4^- in the case of resonances for which the spins were known (up to ~ 400 eV) [2, 4].

The correlation observed between $\langle k \rangle$ and resonance spin was confirmed by the results of the multiplicity spectra calculations performed with a gamma-cascade model of the decay of the compound states and statistical modelling of the detector response function for typical ^{147}Sm resonances with spins of 3^- and 4^- . In order to achieve the statistical modelling a program was set up which applied the Monte Carlo method to calculate the passage of gamma quanta through the detector, taking into account the successive interactions between the gamma quanta and the materials of the detector and its shield, until they were

registered by one of the detector sections. In order to represent the gamma cascade arriving at the entrance to the detector, we used gamma-cascade models, theoretical descriptions of strength functions and the available experimental information on the diagram for the low-lying levels of the corresponding compound nucleus, as described and tested earlier in Ref. [5]. This method, based on experimentally determined multiplicity values, made it possible to obtain a representation of the initial, so-called "physical" multiplicity ν .

The calculation results obtained for ^{147}Sm are shown in Figs 7 and 8. From these it follows that the correlation between the average multiplicity and the spin for the "physical" multiplicity is similar to, but even more pronounced than in the case of the gamma-ray multiplicity observed experimentally.

The existence of this correlation between spin and $\langle k \rangle$ made it possible to determine the spins of some 100 resonances of ^{147}Sm in the 15-900 eV energy range. For the majority of the resonances where the spins were already known, the values were confirmed. However for five resonances (161.0; 161.8; 359.2; 362.3 and 412.0 eV) different spins were obtained. For the 65.1 and 257.0 eV resonances it was found that $\langle k \rangle$ has an intermediate value, and it was also observed that $\langle k \rangle$ was energy-dependent within the limits of the resonances. Thus, $\langle k \rangle$ varies from values corresponding to a spin of 3^- to values corresponding to a spin of 4^- (Fig. 9). This indicates that the 65.1 and 257.0 eV resonances are previously unresolved dual resonances with different spins.

The measurements also showed that the 94.9 eV resonance belongs to the ^{148}Sm isotope, and not to ^{147}Sm .

The determination of $\langle k \rangle$ for resonances of the ^{148}Sm isotope gave a value of ~ 2.5 , which is significantly lower than for ^{147}Sm , where it is found in the range from ~ 3.3 to 3.8 (Fig. 6). No separation of the resonances into groups is observable for the ^{148}Sm isotope.

(b) Neutron and radiation widths

Simultaneous measurements of time-of-flight spectra for neutron capture and scattering made it possible to estimate the neutron and radiation widths of a significant number of resonances. This was done using expressions for the areas under the resonance peaks - S_n in the neutron scattering spectrum and S_γ in the capture gamma-ray spectrum for all multiplicities from 1 to 7:

$$\begin{aligned} S_n &= F(E) \cdot \epsilon_n \cdot A\Gamma_n/\Gamma \\ S_\gamma &= F(E) \cdot \epsilon_\gamma \cdot A\Gamma_\gamma/\Gamma \end{aligned} \quad (1)$$

and their ratio:

$$S_n/S_\gamma = \epsilon_n/\epsilon_\gamma \cdot \Gamma_n/\Gamma_\gamma, \quad (2)$$

where $F(E)$ is the neutron flux of the resonance energy E for a single energy range during measurement of the whole sample area; ϵ_n and ϵ_γ are the counting efficiencies for neutron scattering and capture events, respectively; and A is the area corresponding to the resonance dip in the transmission curve.

In the case of ^{147}Sm , the product of $F(E)\epsilon$ was normalized with respect to the resonances with known parameters in the 18-58 eV range. The energy dependence of the flux has already been measured [6] and in addition was checked against the known ^{238}U resonances. For the unknown resonance parameters of ^{148}Sm , $F(E)\epsilon$ was normalized with respect to the number of counts per channel N^{max} at the 95 eV resonance maximum, for

which the sample in question appeared almost "black" (as shown below, $n\sigma_0 \sim 8$). The correlation used was:

$$S_\gamma/N_\gamma^{\max} = S_n/N_n^{\max} = a/\Delta E \quad , \quad (3)$$

where ΔE is the time channel width in eV.

The efficiency ratio $\epsilon_n/\epsilon_\gamma$ which appears in expression (2) was found from experiments using isotopes with known Γ_n and Γ_γ widths. In view of the detector's high gamma-ray recording efficiency and the high efficiency of the n - γ converter, it was assumed that ϵ_γ and ϵ_n hardly change from resonance to resonance, and that ϵ_n is also not dependent on the scattering material of the target.

In the case of ^{147}Sm , the first five resonances were used in order to determine $\epsilon_n/\epsilon_\gamma$. For ^{148}Sm , owing to the fact that its neutron binding energy and the average number of gamma quanta in the cascade are significantly lower than for ^{147}Sm , the efficiency ratio was also determined from measurements with ^{238}U , for which the $\langle k \rangle$ value of 2.4 and the binding energy are considerably closer to the same values for ^{148}Sm . The difference in the $\epsilon_n/\epsilon_\gamma$ ratio for ^{148}Sm and ^{238}U due to the difference in ϵ_γ was calculated to be 10%. On the basis of the calculations and experimental data, it was assumed that $\epsilon_n/\epsilon_\gamma = 0.55 \pm 0.06$.

Once the product $F(E)\epsilon$ and the ratio $\epsilon_n/\epsilon_\gamma$ were known, the resonance widths were determined on the basis of expressions (1)-(3) and the known dependences of $A\Gamma_n/\Gamma$ and $A\Gamma_\gamma/\Gamma$ on Γ_n and Γ_γ . Since the main concern in the case of ^{147}Sm was to determine Γ_γ , and Γ_n was already known [2], the values for Γ_γ for most resonances were found using the much simpler expression (2).

The determination of the resonance parameters involved making corrections to S_γ and S_n to allow for the contributions made by the recording of capture events in the scattering

channel (4%) and of scattering events in the capture channel (from 5% to 15% depending on the neutron energy). A correction was also made to take account of the capture of neutrons at the target after they had been scattered by the target nuclei. The size of the corrections was determined through special experiments or by calculation.

In processing the measurement results, we also took into account the contribution of impurities caused by the other samarium isotopes contained in the samples in addition to the main isotope, one of these being ^{149}Sm , for which analogous measurements have been performed. The results obtained for this isotope will be published later once they have been processed.

Using the method described above, we obtained Γ_γ for 25 resonances of ^{147}Sm in the 15-300 eV energy range (Table 2) and the widths Γ_n and Γ_γ for a number of ^{148}Sm resonances (Table 3).

The inclusion of a new parameter - gamma-ray multiplicity - in our studies of the radiative capture of resonance neutrons using the multiplicity spectrometry method enabled us to identify ^{147}Sm resonances in terms of spin and to determine previously unknown spin values for a number of resonances of this isotope in the 400-900 eV energy range. In turn, this made it possible to determine more accurately the neutron strength functions for resonances having different spins, which in the 15-600 eV range were found to be $S_0(3) = (6.2 \pm 1.6-1.1) \times 10^{-4}$ for $J = 3$ and $S_0(4) = (3.0 \pm 0.6-0.9) \times 10^{-4}$ for $J = 4$, the difference in strength functions being largely accounted for by the 300-600 eV energy range. The values for $S_0(3)$ and $S_0(4)$ in the energy range up to 300 eV agree fairly well with the results obtained in Ref. [4].

Determination of the radiation widths of the ^{147}Sm resonances showed that Γ_γ varies only slightly from resonance to resonance without going beyond the limits of the measurement errors. Thus, the large fluctuations in Γ_γ described in Ref. [2] cannot be confirmed. An average value of $\langle \Gamma_\gamma \rangle = (75 \pm 4)$ MeV was found for resonances with different spins, together with values for $\langle \Gamma_\gamma \rangle$ which, within the limits of error, proved to be identical.

For ^{148}Sm , we determined the position of more than 20 resonance levels in the energy range up to 3 keV. For a range in which there are evidently no missing levels, we found an average distance between levels of $D_0 = (109 \pm 10)$ eV and a strength function $S_0(3.2 \pm 1.0-2.5) \times 10^{-4}$ which agrees well with the values for S_0 in this range of mass numbers.

For radiation widths of the levels for ^{148}Sm , the average value obtained was $\langle \Gamma_\gamma \rangle \sim 45$ MeV. This is considerably lower than for other samarium isotopes and is one of the lowest for the nuclei in this mass range.

REFERENCES

- [1] MURADYAN, G.V., At. Ehnerg. 50 (1981) 394-398 [in Russian]; Nucl. Sci. Eng. 90 (1985) 60-74.
- [2] MUGHABHAB, S.F., Neutron Cross Sections. 2 Part 3 (1984).
- [3] GEORGIEV, G., et. al., Report by Joint Nucl. Res. Inst., Dubna, P3-88-555 (1988). JANEVA, N., et. al., Nucl. Instr. and Meth. Phys. Res. A. A313 (1992) 266-278 [in Russian].
- [4] KARZHAVINA, Eh.N., KIM SEK SOO, POPOV, A.B., Joint Nucl. Res. Inst. Preprint P3-6237, Dubna (1972) [in Russian].

- [5] GEORGIEV, G., MADZHARSKIJ, T., et. al., *Yad. Ehnerg.* 31 (1981) [in Russian].
- [6] GOLIKOV, V.V., et. al., *Joint Nucl. Res. Inst. Preprint 3-5736, Dubna* (1971) [in Russian].

Table 1

Sample	Isotopic composition of the samples, %						Thickness	
	147	148	149	150	152	154	10^{-5} at/b	
^{147}Sm	96,4	2,3	0,6	0,2	0,4	0,1	34,5	8,62
^{148}Sm	3,3	92,3	3,4	0,4	0,4	0,2	33,0	8,25

Table 2. Resonance parameters for ^{147}Sm

№	E, eV	$\langle k \rangle$	J	Γ_γ , MeV
1	18,36 (2)	3,682 (3)	4	
2	27,16 (2)	3,438 (5)	3	84 (4)
3	29,76 (2)	3,401 (4)	3	71 (4)
4	32,14 (2)	3,667 (3)	4	70 (5)
5	39,70 (2)	3,686 (4)	4	68 (4)
6	40,72 (3)	3,385 (13)	3	
7	49,36 (2)	3,670 (5)	4	75 (4)
8	58,09 (2)	3,400 (4)	3	77 (5)
9	65,10 (3)	3,45 (3)	3	
10	65,10 (3)	3,66 (3)	4	
11	76,15 (3)	3,664 (6)	4	74 (5)
12	79,89 (3)	3,670 (15)	4	
13	83,60 (4)	3,365 (5)	3	76 (5)
14	99,54 (4)	3,605 (7)	4	79 (5)
15	102,69 (4)	3,385 (6)	3	76 (7)
16	106,93 (4)	3,655 (7)	4	82 (5)
17	108,58 (5)	3,710 (35)	4	
18	123,71 (4)	3,370 (6)	3	73 (6)
19	140,00 (4)	3,472 (8)	3	
20	143,27 (5)	3,703 (32)	4	
21	151,54 (5)	3,317 (7)	3	75 (5)
22	161,03 (5)	3,42 (2)	3	
23	161,88 (15)	3,61 (2)	4	
24	163,62 (5)	3,598 (10)	4	77 (4)
25	171,80 (5)	3,668 (14)	4	69 (4)
26	179,68 (6)	3,406 (26)	3	
27	184,14 (5)	3,304 (12)	3	
28	191,07 (5)	3,390 (14)	3	79 (5)
29	193,61 (7)	3,643 (35)	4	
30	198,03 (6)	3,419 (18)	3	61 (4)

№	E, eV	<k>	J	Γ_γ , MeV
31	206,03 (6)	3,564 (8)	4	83 (5)
32	221,65 (6)	3,382 (12)	3	67 (6)
33	225,28 (6)	3,395 (12)	3	86 (5)
34	228,53 (10)	3,636 (45)	4	
35	240,76 (7)	3,700 (21)	4	91 (6)
36	247,62 (7)	3,558 (10)	4	69 (6)
37	257,13 (8)	3,41 (3)	3	
38	257,13 (8)	3,58 (3)	4	
39	263,57 (9)	3,396 (20)	3	
40	266,26 (8)	3,578 (20)	4	72 (6)
41	270,72 (9)	3,405 (15)	3	85 (6)
42	274,40 (10)	3,402 (25)	3	
43	283,28 (10)	3,681 (22)	4	58 (10)
44	290,10 (10)	3,53 (2)	(4)	68 (6)
45	308,3 (2)	3,37 (8)	3	
46	312,06 (12)	3,62 (4)	4	
47	321,13 (18)	3,25 (10)	3	
48	330,1 (2)	3,38 (11)	3	
49	332,1 (3)	3,72 (12)	4	
50	340,4 (2)	3,63 (9)	4	
51	349,86 (18)	3,36 (6)	3	
52	359,32 (15)	3,42 (3)	3	
53	362,15 (35)	3,57 (5)	4	
54	379,2 (2)	3,331 (17)	3	
55	382,4 (3)	3,402 (21)	3	
56	390,5 (2)	3,68 (4)	4	
57	396,5 (3)	3,47 (3)	(3)	
58	398,6 (3)	3,34 (3)	3	
59	405,1 (2)	3,416 (30)	3	
60	412,0 (2)	3,38 (3)	3	
61	418,3 (2)	3,42 (2)	3	
62	421,8 (3)	3,63 (5)	4	
63	435,7 (3)	3,29 (3)	3	
64	440,2 (3)	3,66 (4)	4	
65	446,9 (3)	3,45 (8)	(3)	
66	458,6 (3)	3,66 (3)	4	
67	462,9 (3)	3,40 (4)	3	
68	476,0 (3)	3,58 (5)	4	
69	479,8 (3)	3,32 (4)	3	

No	E, eV	$\langle k \rangle$	J	Γ_γ , MeV
70	486,4 (3)	3,43 (4)	3	
71	496,2 (4)	3,46 (4)	(3)	
72	498,6 (4)	3,32 (4)	3	
73	513,5 (3)	3,42 (2)	3	
74	528,9 (4)	3,62 (8)	4	
75	532,5 (4)	3,40 (10)	(3)	
76	538,1 (3)	3,38 (4)	3	
77	546,0 (4)	3,46 (4)	(3)	
78	553,2 (πB)	3,34 (6)	3	
79	559,7 (4)	3,29 (6)	3	
80	563,4 (4)	3,55 (5)	(4)	
81	574,3 (4)	3,62 (5)	4	
82	580,2 (5)	3,27 (5)	3	
83	587,8 (4)	3,35 (5)	3	
84	597,4 (4)	3,59 (4)	4	
85	606,0 (4)	3,68 (5)	4	
86	617,2 (5)	3,45 (4)	(3)	
87	634,0 (4)	3,42 (6)	3	
88	659,5 (4)	3,55 (6)	(4)	
89	668,8 (4)	3,77 (6)	4	
90	697,0 (4)	3,60 (4)	4	
91	714,0 (5)	3,37 (4)	3	
92	744,3 (5)	3,67 (6)	4	
93	796,2 (5)	3,34 (7)	3	
94	808,0 (5)	3,37 (4)	3	
95	821,0 (5)	3,39 (9)	3	
96	836,1 (5)	3,54 (4)	(4)	
97	875,2 (6)	3,36 (4)	3	
98	896,1 (6)	3,26 (6)	3	

Table 3. Resonance parameters for ^{148}Sm

E, eV	Γ_n , MeV	Γ_n^0 , MeV	Γ_γ , MeV
94,9 (1)	385 (35)	39,5 (3,6)	60 (10)
140,2 (1)	34 (4)	2,9 (0,4)	43 (8)
184,4 (1)	780 (70)	57,5 (5,2)	53 (8)
288,2 (1)	410 (40)	24,2 (2,4)	51 (10)
422,0 (2)	208 (20)	10,1 (1,0)	43 (7)
513,5 (2)	735 (70)	32,4 (3,2)	41 (10)
557,4 (3)	92 (15)	3,9 (0,6)	42 (10)
622,9 (3)	580 (50)	23,2 (2,0)	40 (10)
883,1 (4)	1050 (15 0)	35,3 (5,0)	53 (20)
909,6 (5)	2400 (300)	79,6 (9,9)	
1010 (1)			
1157 (1)			
1180 (1)			
1385 (2)	500 (80)	13,4 (2,1)	
1478 (2)	1450 (200)	37,7 (5,2)	
1638 (3)			
1699 (2)			
1860 (3)			
1960 (3)			
2053 (3)			
2145 (5)			
2207 (5)			
2306 (6)			
2415 (6)			
2955 (8)			

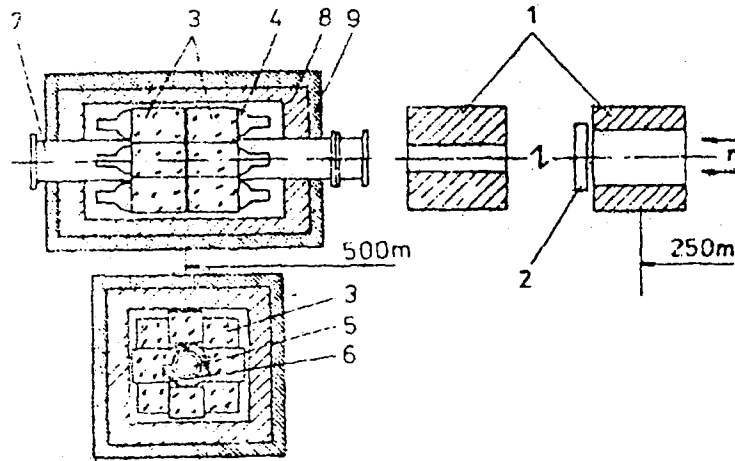


Fig. 1. Longitudinal and lateral sections of the multisection gamma scintillation detector: 1 - collimator, 2 - filter, 3 - NaI(Tl) crystals, 4 - photomultiplier - 110, 5 - sample, 6 - converter, 7 - vacuumized channel for positioning of sample, 8 - lead shield, 9 - shield made of B₄C with paraffin.

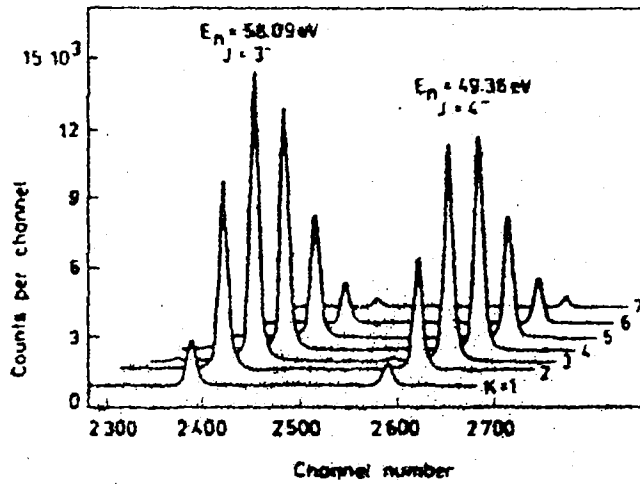


Fig. 2. Part of the time-of-flight coincidence spectra for different multiplicities k for ¹⁴⁷Sm capture gamma rays.

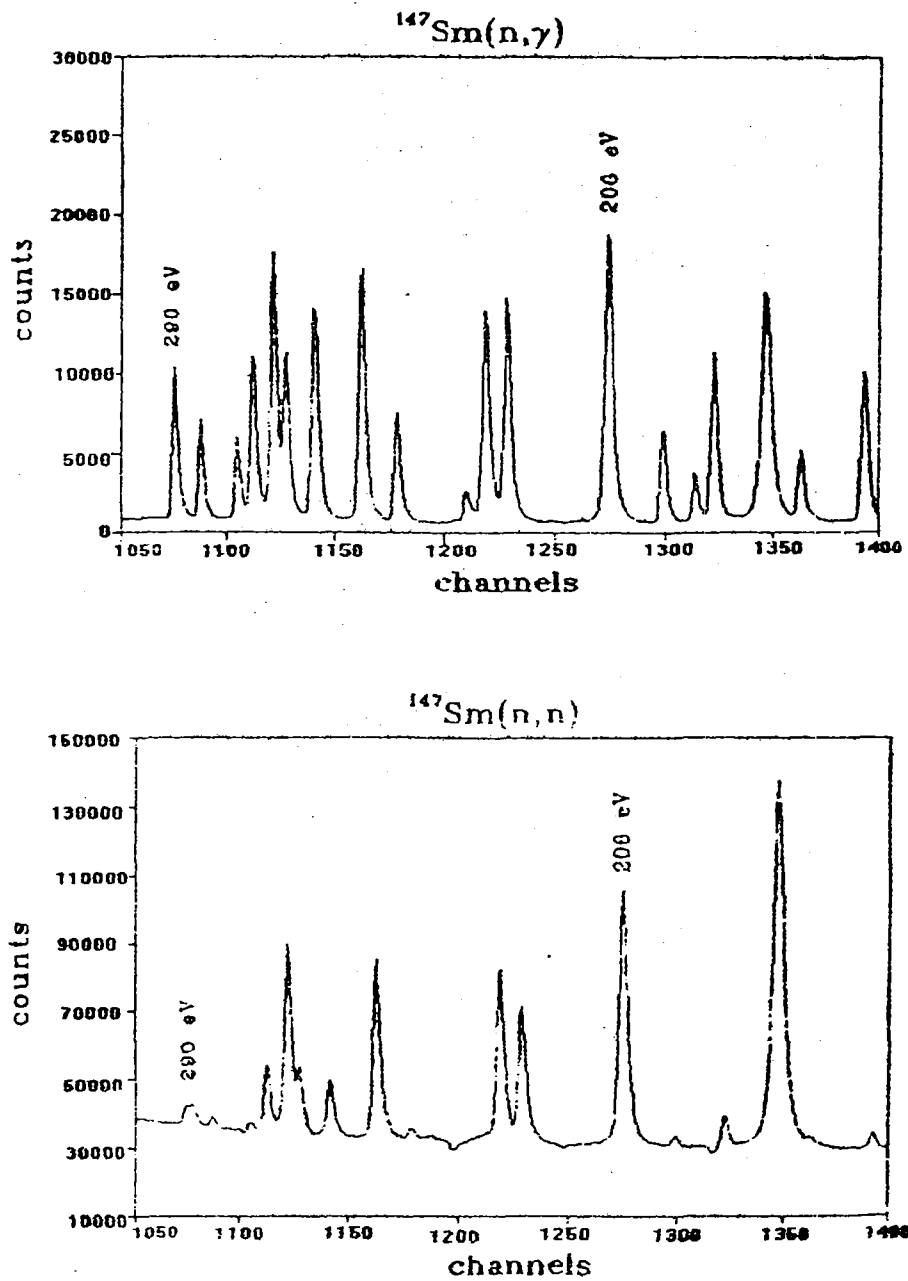


Fig. 3. Part of the time-of-flight spectrum for (a) quadruple coincidences of capture gamma rays and (b) neutron scattering events for a ^{147}Sm sample with a thickness of 3.45×10^{-4} at/b.

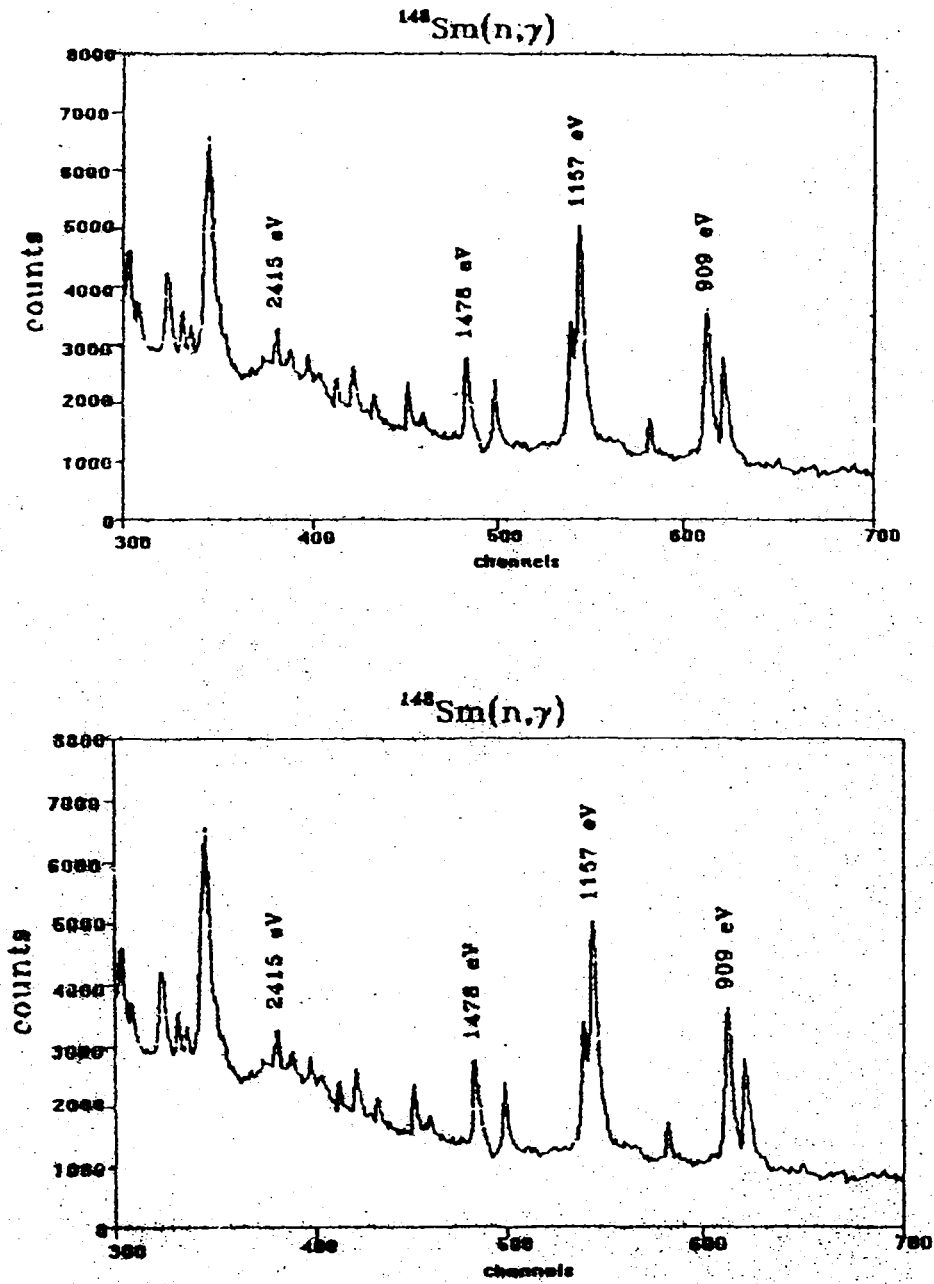


Fig. 4. Time-of-flight spectra for (a) triple coincidences of capture gamma rays and (b) neutron scattering events for a ^{148}Sm sample with a thickness of 3.3×10^{-4} at/b. The small peaks are the result of ^{147}Sm and ^{149}Sm impurities.

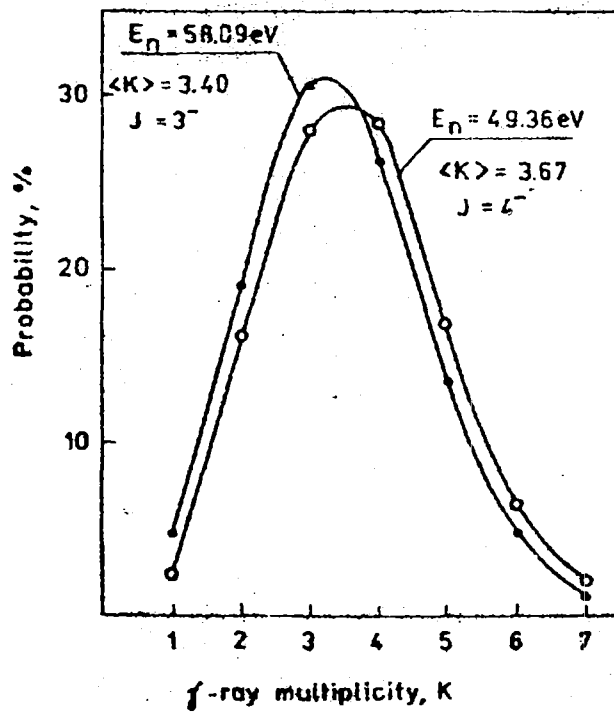


Fig. 5. Experimental multiplicity distribution for capture gamma ray for two ^{147}Sm resonances with different spins.

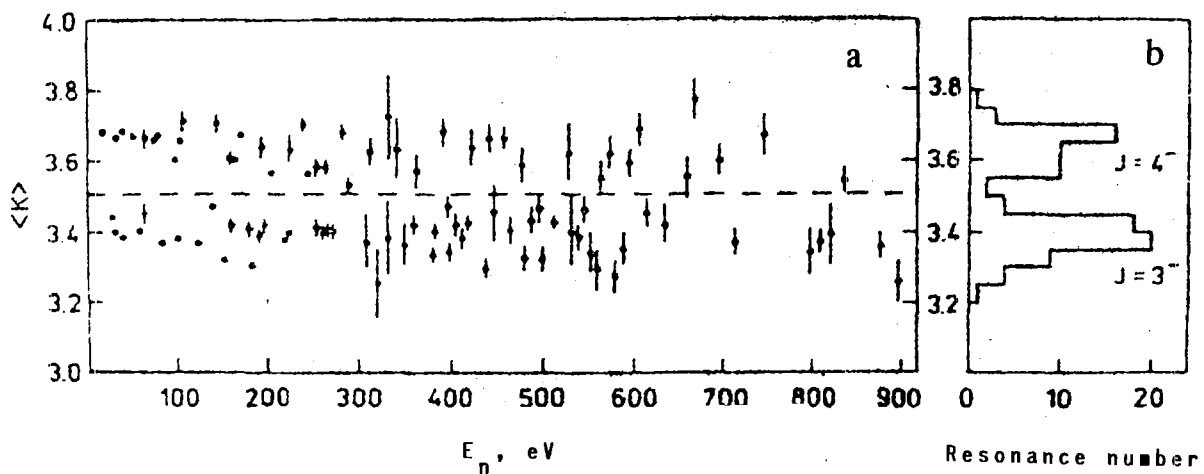


Fig. 6. (a) Experimental values for the average multiplicity $\langle k \rangle$ of capture gamma rays for ^{147}Sm resonances.
 (b) Number of resonances in the range $\Delta \langle k \rangle = 0.05$ as a function of $\langle k \rangle$.

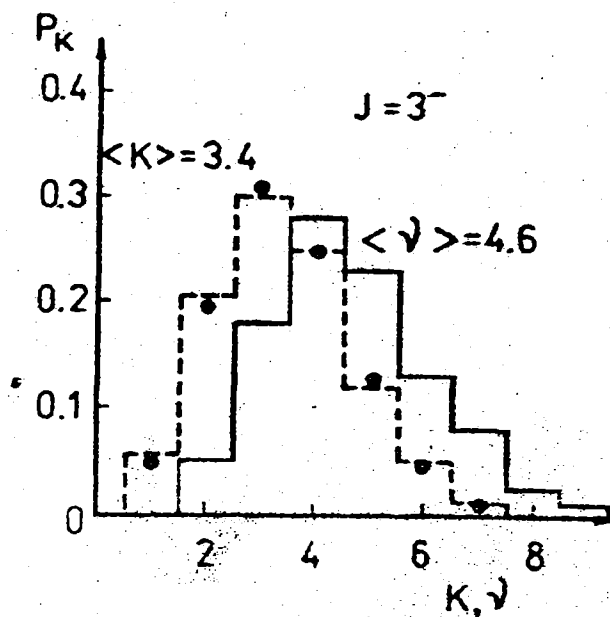


Fig. 7. Calculated multiplicity distributions for capture gamma rays for ^{147}Sm resonances with a spin $J = 3^-$:
 ——— calculated distribution of the "physical" multiplicity - ν ;
 - - - - - calculated distribution of the detector coincidence multiplicity - k ;
 • experimental multiplicity distribution

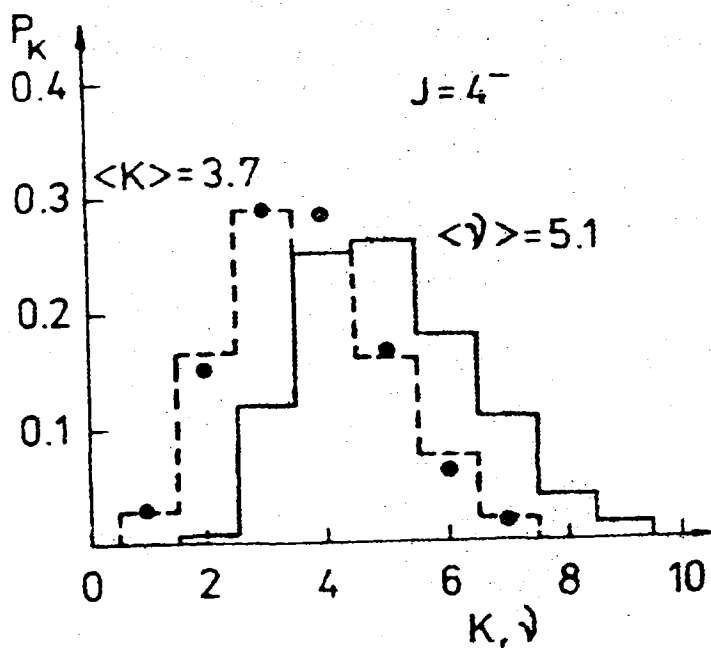


Fig. 8. Calculated multiplicity distributions for capture gamma rays for ^{147}Sm resonances with a spin of $J = 4^-$ (for key see Fig. 7).

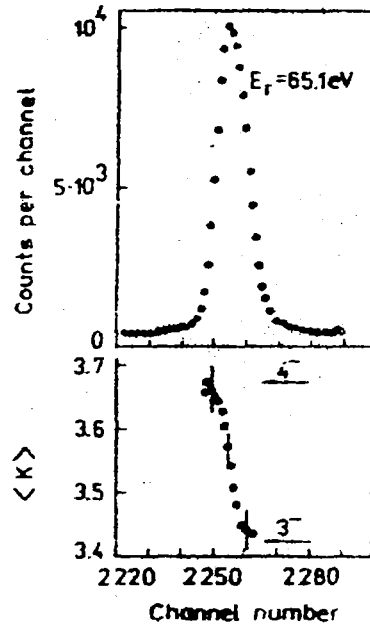


Fig. 9. Specification by channel of average multiplicity $\langle k \rangle$ in the 65 eV resonance region for ^{147}Sm .
A slight variation in $\langle k \rangle$ can be seen between the values which are characteristic for resonances with a spin of 4^- and those which are characteristic for resonances with a spin of 3^- .